Neurotox Res (2015) 28:209–221
DOI 10.1007/s12640-015-9538-8

ORIGINAL ARTICLE

Cobalt-Induced Ototoxicity in Rat Postnatal Cochlear Organotypic Cultures

Peng Li[1] · Dalian Ding[2,3] · Richard Salvi[1] · Jerome A. Roth[4]

Received: 28 May 2015 / Revised: 28 June 2015 / Accepted: 30 June 2015 / Published online: 8 July 2015

Abstract Cobalt (Co) is a required divalent metal used in the production of metal alloys, batteries, and pigments and is a component of vitamin B12. Excessive uptake of Co is neurotoxic causing temporary or permanent hearing loss; however, its ototoxic effects on the sensory hair cells, neurons, and support cells in the cochlea are poorly understood. Accordingly, we treated postnatal day 3 rat cochlear organotypic cultures with various doses and durations of $CoCl_2$ and quantified the damage to the hair cells, peripheral auditory nerve fibers, and spiral ganglion neurons (SGN). Five-day treatment with 250 μM $CoCl_2$ caused extensive damage to hair cells and neurons which increased with dose and treatment duration. $CoCl_2$ caused greater damage to outer hair cells than inner hair cells; damage was greatest in the base of the cochlea and decreased towards the base. $CoCl_2$ increased expression of superoxide radical in hair cells and SGNs and SGN loss was characterized by nuclear condensation and fragmentation, morphological features of apoptosis. $CoCl_2$ treatment increased the expression of caspase-3 indicative of caspase-mediated programmed cell death. These results identify hair cells and spiral ganglion neurons as the main targets of Co ototoxicity in vitro and implicate the superoxide radical as a trigger of caspase-mediated ototoxicity.

Keywords Cobalt · Cochlea · Hearing · Apoptosis · Hair cells · Acoustic neurons

✉ Jerome A. Roth
jroth@buffalo.edu

[1] Department of Otolaryngology Head and Neck Surgery, The Third Affiliated Hospital of Sun Yat-Sen University, Guang Zhou 510630, China

[2] Center for Hearing and Deafness, University at Buffalo, Buffalo, NY 14214, USA

[3] Department of Otolaryngology Head and Neck Surgery, Xiangya Hospital, Central South University, Changsha 410008, Hunan, China

[4] Department of Pharmacology and Toxicology, University at Buffalo, 11 Cary Hall, Buffalo, NY 14214, USA

Introduction

Cobalt (Co), a required divalent metal expressed ubiquitously in the environment, is widely used in the production of metal alloys, batteries, and blue pigment for the coloration of glass and paints. Co is essential for human health because it is a part of vitamin B12 complex where it functions in the production of red blood cells, synthesis, and regulation of DNA and fatty acid and amino acid metabolism. The required daily intake of Co is 2.4 μg/day although the total daily intake is higher and estimated to be between 5 and 40 μg/day. Gastrointestinal absorption is relatively low ranging from 5 to 45 % and largely dependent on the solubility of the composition of Co ingested. A major portion of absorbed Co is bound to serum albumin and other serum proteins and is readily eliminated in the urine unless complexed to the corrin ring system in vitamin B12 (Yamada 2013; Simonsen et al. 2012).

Based on its toxicity and long-term stability in the environment as well as its high probability score, a study by the Department of Defense rated $CoCl_2$ as having the highest toxicity potential among a subclass of 36 pure elements and metal compounds used in industry including toxic compounds such as arsenic, lead oxide, mercuric nitrate, mercury, and cadmium (Sutto 2011; Permenter et al. 2013). The LD50 value for soluble Co salts has been estimated to be

between 150 and 500 mg/kg. Humans are typically exposed to Co through diet, inhalation, or dermatological exposure with soil or water. Acute and chronic exposure to high levels of Co by inhalation results in respiratory dysfunction, reflected in a significant reduction in ventilator performance, congestion, edema, and hemorrhage, and medical conditions such as asthma, pneumonia, and fibrosis (Simonsen et al. 2012; Swennen et al. 1993; Rehfisch et al. 2012). Additional deleterious consequences from chronic exposure include dysfunctions of heart, liver, kidney, conjunctiva, thyroid, immune system, vision, and hearing.

The toxicological properties of Co has recently come to the forefront from a number of studies indicating that chronic exposure to Co particles caused by the wearing away of metal-on-metal hip implants leads to a severe disorder, called metallosis characterized by weight loss, heart and thyroid dysfunction, blindness, and peripheral neuropathy including sensory disturbance with severe hearing loss (Meecham and Humphrey 1991; Ikeda et al. 2010; Pelclova et al. 2012; Apostoli et al. 2013). Patients with malfunctioning hip implants have serum Co concentrations 100-fold greater than normal physiologic levels. One of the most recurrent adverse outcomes associated with failing metal-on-metal implants as well as occupational exposures to Co is hearing loss. The precise mechanisms underlying Co-induced hearing loss has received limited attention although rabbits intravenously exposed to Co display a time and dose-dependent degeneration of the organ of Corti with loss of both the inner (IHC) and outer hair cells (OHC) as well as degeneration of the spiral ganglion (Apostoli et al. 2013). However, no mention was made of a tonotopic gradient of cochlear pathology characteristic of most ototoxic drugs, possible damage to the stria vascularis, potential mechanisms triggering cell death, or functional assessment of hearing deficits. Other studies using cochlear organotypic cultures from postnatal day 4 rats demonstrated that high doses of $CoCl_2$ induced swelling of hair cells, accompanied by hair cell loss (Lee et al. 2013; Battaglia et al. 2009). However, these studies failed to note whether there was preferential loss of OHC versus IHC, a tonotopic gradient of hair cell loss or degeneration of auditory nerve fibers (ANF) or spiral ganglion neurons (SGN), the latter being important because Co is considered highly neurotoxic (Mates et al. 2010).

The mechanisms and pathways, apoptosis or necrosis, leading to Co-induced degeneration of cochlear hair cells and/or neurons are poorly understood. Recent studies suggest that Co toxicity may be initiated by mitochondrial dysfunction as Co can induce ROS formation (Jomova and Valko 2011) and modify the mitochondrial permeability transition pore leading to mitochondrial swelling, electrical membrane potential collapse (Battaglia et al. 2009), and eventual apoptotic cell death. To more fully elucidate the cell types and mechanisms underlying Co-induced ototoxicity, we treated rat postnatal day 3 cochlear organotypic cultures with various doses and durations of $CoCl_2$. Since our cultures contain the entire length of the cochlea, we were able to determine if Co is more toxic to OHC than IHC, if there is a base to apex gradient of hair cell loss and if Co is more toxic to hair cells than ANF and SGN. Fluorescent probes were also used to test for Co-induced generation of the highly toxic superoxide anion and caspase-3-mediated cell death.

Materials and Methods

Animals

Postnatal day 3 Sprague–Dawley rat pups purchased from Charles River Laboratories (Wilmington, MA) were used as subjects. All experimental procedures were approved by the Institutional Animal Care and Use Committee (IACUC) of University at Buffalo.

Cochlear Organotypic Cultures and Co Treatment

The procedures for preparing cochlear organotypic cultures have been previously described (Ding et al. 2011a, b). Briefly, rat pups were decapitated and the cochlea removed. The entire basilar membrane containing the organ of Corti with hair cells and SGN was micro-dissected out in Hank's Balanced Salt Solution (HBSS, Invitrogen) and placed on the surface of a droplet (15 µl) of freshly prepared rat tail collagen gel (rat tail collagen, 10× basal medium eagle (BME) medium, and 2 % sodium carbonate in a ratio of 9:1:1) on the bottom of a 35-mm tissue culture dish. Cochlear explants were incubated in 1.3 ml of serum-free medium (1× BME plus serum-free supplement, 1 % bovine serum albumin, 2 mM glutamine, and 20 % glucose) in a CO_2 incubator at 37 °C overnight. Cultures were subsequently treated with 2 ml culture medium containing several different concentrations of $CoCl_2$ ($\leq$500 µM) for varying treatment durations ($\leq$8 days). (Note: In preliminary experiments, we did not observe any damage with the highest concentration of $CoCl_2$ after 24 or 48 h treatment; therefore, the results presented below show results for treatment duration between 3 and 8 days.)

Labeling

At the end of the experiment, explants were fixed with 10 % formalin in PBS for 2 h. To label, quantify, and image the SGN and AN, cochlear explants were rinsed with PBS and then immersed overnight in a solution containing 2 µl of mouse anti-β-tubulin III antibody (Covance, TUJ1,

#MMS-435P; 1:100 dilution), 20 µl Triton X-100 (10 %), 6 µl normal goat serum, and 152 µl of 0.01 M PBS. Specimens were rinsed three times in PBS and immersed in a solution containing 2 µl of secondary anti-mouse IgG conjugated with TRITC (Sigma T5393), 12 µl normal goat serum, 40 µl Triton X-100 (10 %), and 346 µl of PBS for 1 h. To label, quantify, and image the stereocilia and cuticular plate of the hair cells, the stereocilia and cuticular plate of the hair cells, specimens were rinsed with PBS and stained with Alexa Fluor 488-conjugated phalloidin (1:100×, Invitrogen A12379) for 40 min. To stain the nuclei, specimens were stained with 1 µM To-PRO-3 (Invitrogen T3605) for 30 min. Specimens were then rinsed in PBS, mounted on glass slide in glycerin, cover slipped, and examined with a confocal microscope (Zeiss LSM-510) with appropriate filters for TRITC (absorption: 544 nm, emission: 572 nm), Alexa Fluor 488 (excitation 495 nm, emission 519 nm), and To-PRO-3 (excitation 642 nm, emission 661 nm). Images were evaluated with Zeiss LSM image Examiner and post-processed with Adobe Photoshop software. These triple stained specimens were used to image and quantify hair cells, SGN and ANF. A total of 72 cochlear organotypic cultures were used for these studies; 72 were used for hair cell counts, 48 for ANF counts, and 48 for SGN counts.

Superoxide Formation

In the presence of superoxide, dihydroethidium is oxidized to fluorescent ethidium which bind to nuclear DNA and RNA (Deng et al. 2013; Nicotera et al. 2004). Dihydroethidium (Sigma D7008) was used to detect superoxide expression in cochlear cultures treated for 3 days with 250 or 500 µM $CoCl_2$. Cochlear cultures were incubated with 100 nM dihydroethidium for 30 min and then fixed for 2 h with 10 % formalin in PBS. Cultures were then stained with Alexa Fluor 488-conjugated phalloidin for 30 min, while nuclei were stained with 0.75 µM To-PRO-3 for 20 min as described above and examined with a confocal microscope (Zeiss LSM-510) using appropriate filters to detect fluorescent ethidium (absorption: 544 nm, emission: 572 nm), Alexa Fluor 488-conjugated phalloidin (excitation 495 nm, emission 519 nm), and TO-PRO-3 (excitation 642 nm, emission 661 nm). Confocal images were evaluated with Zeiss LSM Image Examiner software and images post-processed with Adobe Photoshop. The ethidium fluorescent signal reflecting superoxide was quantified using ImageJ software (ver. 1.46j) as follows. The image files were split into three channels (Green, Red, and Blue) using Image/split channels. The red image, representing superoxide, was chosen and from the analyze menu; the function "measure" was used to obtain values of integrated intensity in the designated area, namely the hair cell region (HCR) and SGN region. In each sample, mean values of background intensity were subtracted to obtain the final values. Mean values of integrated intensity/area were determined for each group ($n = 5$ cochlea cultures) and used to compute the average superoxide level. A total of 15 cochlear cultures were used for the superoxide studies.

Caspase-3

To evaluate caspase-3 activity in live cells a cell membrane permeable fluorogenic substrate, Red-IETD-FMK caspase-3 (BioVision Lot 70693) was used to label the activated caspase-3 in cochlear cultures treated with 0 (control), 250, or 500 µM $CoCl_2$ ($n = 15$/condition) using procedures described previously (Ding et al. 2007, 2010; Wang et al. 2014). At the end of the experiment, cochlear explants were incubated with Red-IETD-FMK caspase-3 at a dilution of 1:200 for 1 h. Afterwards, the explants were fixed in 10 % formalin in PBS at 4 °C overnight and then co-labeled with Alexa Fluor 488-conjugated β-tubulin antibody, To-PRO-3, or Alexa Fluor 488-conjugated phalloidin as described above. Samples were examined with a confocal microscope (Zeiss LSM-510) using appropriate filters to detect caspase-3, phalloidin, TO-PRO-3, and β-tubulin. Confocal images were evaluated with Zeiss LSM Image Examiner software and images post-processed with Adobe Photoshop. A total of 15 cochlear organotypic cultures were used for the caspase-3 studies.

Cochleograms

To quantify the hair cell degeneration induced by $CoCl_2$, phalloidin-labeled IHC and OHC were counted over the entire length of the cochlea under a fluorescent microscope (Zeiss Axioskop, ×400) equipped with appropriate filters as described previously (Qi et al. 2008; Ding et al. 2011a, b). The observer making the hair cell counts was unaware of the experimental treatment. Hair cells were counted as missing if the stereocilia were absent and the cuticular plate was damaged. Using laboratory norms, a cochleogram was constructed for an explant by plotting the percent hair cell loss as a function of the percent distance from the apex of the cochlea. For quantitative analysis, individual cochleograms were grouped to generate a mean cochleogram for each treatment condition using custom software.

Quantification of ANF

To quantify the degeneration of ANF, the numbers of ANF projecting towards the hair cells in the organ of Corti were counted in the middle turn using a fluorescence microscope equipped with appropriate filters (Zeiss Axioskop, 630×) as previously described (Ding et al. 2013a, b). The

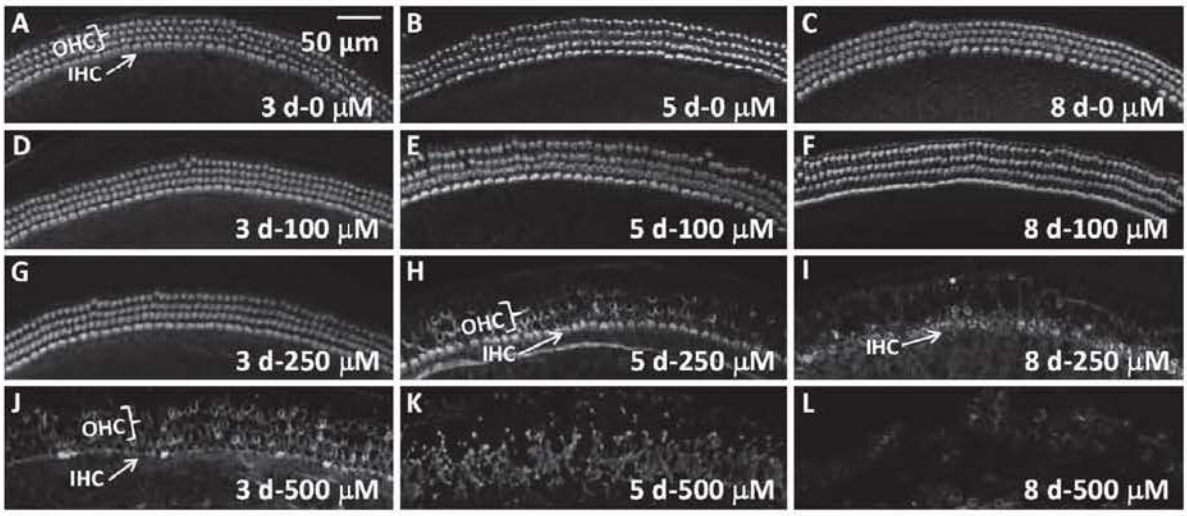

Fig. 1 Representative photomicrographs of cochlear organotypic cultures from the middle turn of the cochlea. Specimens labeled with Alexa 488-conjugated phalloidin which labels the stereocilia bundles and to a lesser extent the cuticular plate at the apical surface of the hair cells. **a–c** Controls cochleae cultured with 0 µM $CoCl_2$ for 3, 5, or 8 days. **d–f** Cochleae cultured with 100 µM $CoCl_2$ for 3, 5, or 8 days. **g–i** Cochleae cultured with 250 µM $CoCl_2$ for 3, 5, or 8 days. **j–l** Cochleae cultured with 500 µM $CoCl_2$ for 3, 5, or 8 days. Outer hair cells (OHC), *bracket*; inner hair cells (IHC), *arrow* (Color figure online)

investigator making the counts was unaware of the experimental condition. ANF were counted (counts obtained over a μm^2; three location assessed in the middle turn), and the mean value was computed for each culture. The number of ANF were calculated in four explants per experimental condition ($n = 4$). All statistical analyses were carried out using a one-way ANOVA ($p < 0.05$) followed by Newman–Keuls post hoc analyses using the GraphPad Prism 5 software (Ding et al. 2013b).

Quantification of SGN

As described previously, the numbers of normal SGN (large round soma, large round nucleus) and damaged SGN (shrunken soma, condensed or fragmented nuclei) were counted from each 0.5 µm slice within a confocal image stack [Zeiss LSM Image Examiner software, area: 1.414 μm^2, 0.5 µm per slice, 100–200 µm thickness, counts obtained from 10 to 20 slices per location, each slice separated by 20 µm to avoid double counting of damaged SGN (Fu et al. 2013; Liu et al. 2014; Ding et al. 2013b)]. The observer making the counts was unaware of the experimental treatment. The values obtained were used to compute the percentage of normal SGN within each region. Measurements were obtained from three locations in the middle turn of each explant and the mean value computed for each culture. Measurements were obtained from four cultures per condition and the data were evaluated using a one-way ANOVA followed by Newman–Keuls post hoc analyses using the GraphPad Prism 5 software ($p < 0.05$).

Results

Hair Cell Loss

Figure 1a–c shows representative photomicrographs taken from the middle turn of cochlear cultures maintained in standard culture medium (0 µM $CoCl_2$) for 3, 5, or 8 days. The stereocilia bundles on the apical surface of the hair cells were heavily labeled with Alex Fluor 488-conjugated phalloidin. The three rows of OHC and one row of IHC were arranged in a gently curving arc with little or no evidence of loss or damage. These results indicate that the hair cells remain intact in control cultures for at least 8 days. The effects of 3-, 5-, or 8-day treatment with 100 µM $CoCl_2$ are shown in Fig. 1d–f, respectively; 100 µM of $CoCl_2$ had no noticeable effect on hair cell integrity even after 8-day treatment. The effects of 3-, 5-, or 8-day treatment with 250 µM $CoCl_2$ are shown in Fig. 1g–i. Hair cells were intact after 3-day treatment. However, at 5 days, there was significant OHC loss and damage, but most IHC were still present. After the 8 days treatment, most OHC were missing; although most IHC were still present, though their stereocilia were damaged or missing. Treatment of cultures with 500 µM $CoCl_2$ for 3 days resulted in moderate to severe damage to both OHC

and IHC (Fig. 1j). After 5 days, essentially all cochlear hair cells in the middle turn were severely damaged or missing and after 8 days all hair cells were missing (Fig. 1l).

Cochleograms

Mean ($n = 6$ cultures/group) cochleogram showing the percentages of missing OHC and IHC as a function of percent distance from the apex of the cochlea were computed for all conditions. The mean cochleograms for controls (0 μM $CoCl_2$) maintained in culture for 3, 5, or 8 days are shown in Fig. 2. There was little evidence of OHC or IHC loss after 3 days in culture except for a very small loss (~9 %) near the extreme base (95 % from apex) and apex (5 % from apex) (Fig. 2a); IHC and OHC losses were similar after 5 and 8 days in culture except that the hair cells lesions in the extreme base (95 % from apex) increased to ~20 % at 5 days and ~35 % at 8 days. The modest increase in hair cell loss at these times likely reflects subtle damage during dissection combined with increased vulnerability of the base of the cochlea due to lower antioxidant enzyme levels in this region (Sha et al. 2001). Mean cochleograms treated with 100 μM $CoCl_2$ for 3, 5, or 8 days (Fig. 2d–f) or 250 μM for 3 days were similar to controls (Fig. 2g). In contrast, cultures treated with 250 μM $CoCl_2$ for 5 days showed a massive increase in OHC loss in the basal half of the cochlea (Fig. 2h). Those treated for 8 days showed almost total loss of OHC and a slight increase in IHC loss in near apex and base of the cochlea (Fig. 2i). The highest dose of $CoCl_2$, 500 μM, caused a complete loss of OHC and IHC after 5 or 8 days of treatment, whereas the 3 days of treatment resulted in 100 % loss of OHC and IHC near the base of the cochlea which declined to <10 % near the apex. Collectively, these results indicate that $CoCl_2$ is more toxic to OHC than IHC and that hair cell loss progresses from the base towards the apex consistent with other ototoxic drugs.

ANF and SGN

ANF and SGN were evaluated in control cultures (0 μM $CoCl_2$) and cultures treated with $CoCl_2$ for 3, 5, and 8 days. Figure 3a–d shows representative photomicrographs from the middle of control cultures and cultures treated with 100, 250, or 500 μM $CoCl_2$ for 8 days; specimens were immunolabeled with an antibody against β-tubulin III which is heavily expressed in the fibers and soma of neurons. In the 8-day control, thick fascicles of ANF can be seen projecting out radially from the SGN to the HCR. The numerous large, round structures of the SGN were heavily labeled with tubulin (Fig. 3a). The ANF and SGN in cultures treated for 8 days with 100 μM $CoCl_2$ were similar to control cultures (Fig. 3b). In contrast, 8-day treatment with 250 mM $CoCl_2$ resulted in substantial loss of ANF and SGN (Fig. 3c); the remaining ANF fascicles were thinner and fragmented and the soma of the residual SGN were generally smaller, ovoid, and misshapen.

Effect of Treatment Duration on ANF

To assess the effects of duration of $CoCl_2$ treatment, we counted the numbers of ANF fascicles (see "Materials and Methods") in the middle turn of four cochlear explants per condition. Approximately 75 ANF/140 μm were present in controls cultured for 3, 5, or 8 days (Fig. 3e); there was no change in the mean numbers of ANF with increasing culture duration (one-way ANOVA, $F = 0.288$; 3, 9 df, $p = 0.756$). Mean ANF counts in cultures treated with 100 μM $CoCl_2$ for 3, 5, and 8 days were 77.2, 72.8, and 74.3, respectively; there was no significant decrease in ANF numbers with increasing treatment duration (one-way ANOVA, $F = 1.27$; 3, 11 df, $p = 0.363$). The 250 μM dose of $CoCl_2$ caused a significant decrease in ANF numbers with increase in treatment duration; mean ANF counts/140 μm were 77.5, 62.8, and 48.8, respectively, for 3-, 5-, and 8-day treatment (one-way ANOVA, $F = 29.7$, 3, 9 df, significant effect of duration, $p < 0.001$). A Newman–Keuls post hoc analysis ($p < 0.05$) showed that ANF counts in 8-day group were significantly less than in 5- or 3-day group and that ANF counts in 5-day group were significantly less than in 3-day group. The 500 μM dose of $CoCl_2$ caused a significant decrease in ANF counts. Mean ANF/140 μM were 18.0, 18.0, and 0 in 3-, 5-, and 8-day treatment groups; there was a significant effect of treatment duration (one-way ANOVA; $F = 31.35$, 3, 11 df, $p < 0.001$). A Newman–Keuls post hoc analysis ($p < 0.05$) indicated that ANF counts in 5- and 8-day treatment groups were significantly different from 3-day group.

ANF Dose–Response

To assess the effect of $CoCl_2$ dose, we compared the mean ANF counts for 3-, 5-, and 8-day treatments (Fig. 4). After 3-day treatment, mean (+SEM) ANF/140 μm were 75.3, 77.3, 77.5, and 18.0 in the control group and groups treated with 100, 250, and 500 μM $CoCl_2$, respectively (Fig. 4a). There was a significant effect of dose (one-way ANOVA, $F = 212.6$, 3, 12 df, $p < 0.0001$). A Newman–Keuls post hoc analysis ($p < 0.05$) indicated that ANF counts in the 500 μM $CoCl_2$ group were significantly less than in the 0, 100, and 250 mM groups. In the case of the 5-day treatment, the mean (+SEM) ANF/140 μm were 75.8, 72.8, 62.8, and 18.0 in the control groups and 100, 250, and 500 μM $CoCl_2$ groups, respectively (Fig. 4b). There was a significant effect of dose (one-way ANOVA, $F = 116.3$, 3,

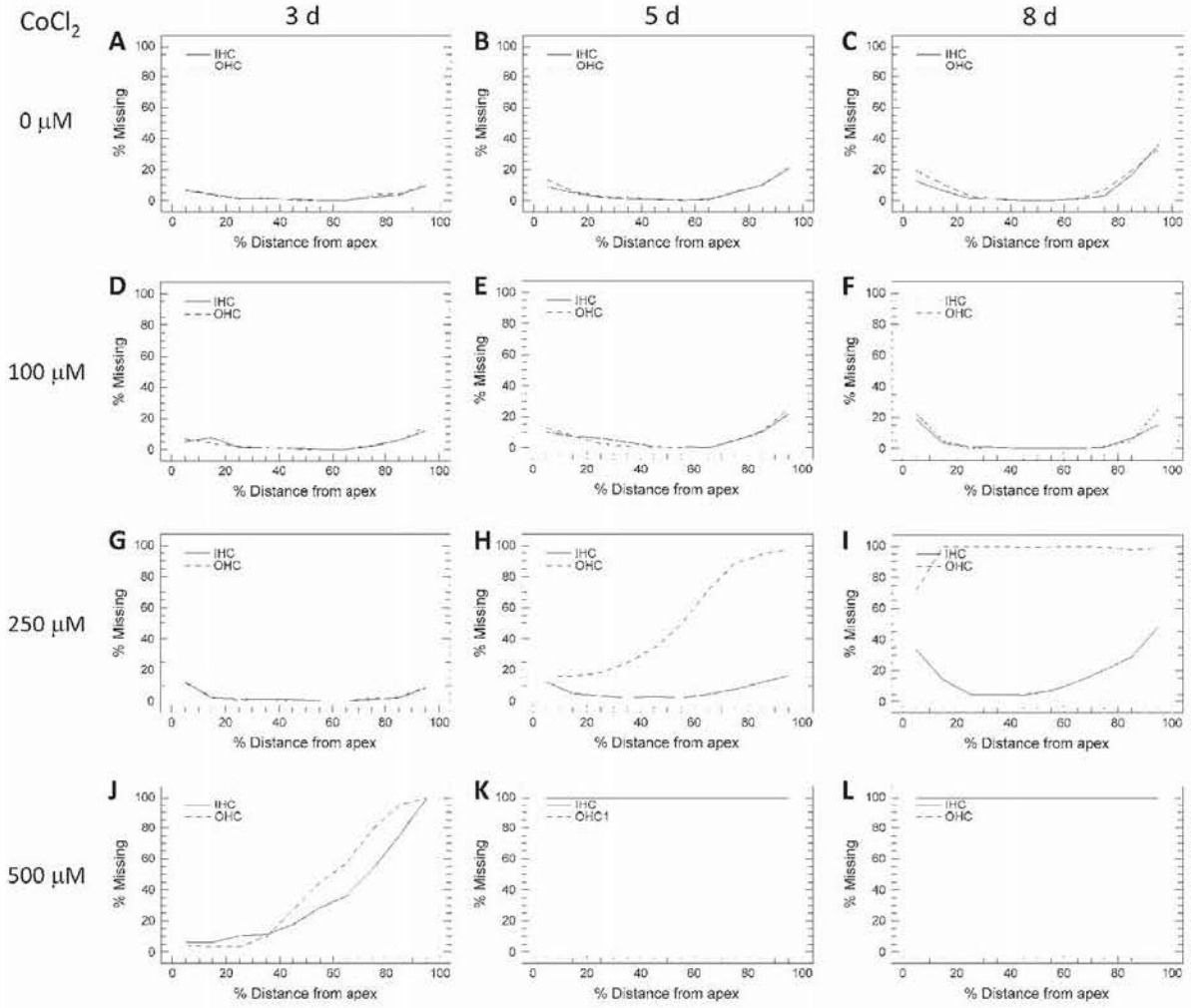

Fig. 2 Mean cochleograms ($n = 6$) showing the percent missing outer hair cells (OHC, *dashed line*) and inner hair cells (IHC, *solid line*) in cochleae cultured for 3, 5, or 8 days without (**a**–**c**) or with 100 μM (**d**–**f**), 250 μM (**g**–**i**), or 500 μM (**j**–**l**) $CoCl_2$

12, df, $p < 0.0001$). A Newman–Keuls post hoc analysis ($p < 0.05$) indicated that ANF counts in the 500 μM group were significantly less than in the 0, 100, and 250 μM groups and that the 250 μM group was significantly less than the 0 μM control group. With 8-day treatment, mean (+SEM) ANF/140 μm in the 0, 100, 250, and 500 μM $CoCl_2$ group were 73.0, 74.3, 48.8, and 0, respectively. There was a significant effect of dose (one-way ANOVA, $F = 182.2$, 3, 12 df, $p < 0.0001$). A Newman–Keuls post hoc analysis ($p < 0.05$) indicated that ANF counts in the 500 μM group were significantly less than in the 0, 100, and 250 μM groups and that ANF counts in the 250 μM group were significantly less than in the 0 and 100 μM groups.

Spiral Ganglion Neurons

Figure 4a–d shows representative photomicrographs of SGN soma cultured for 8 days in 0 (control), 100, 250, and 500 μM $CoCl_2$. The SGN in 0 μM control cultures were characterized by a large, round soma heavily labeled by tubulin and a centrally located nucleus devoid of staining (Fig. 4a). The soma of SGN cultured with 100 μM $CoCl_2$ were similar those in the control group (Fig. 4b). In contrast, there was a large decrease in the density of SGN in the 250 and 500 μM groups, and among the SGN still present, the soma and nucleus of residual neurons tended to be shrunken, distorted, or fragmented, morphological features of cells undergoing apoptosis (Fig. 4c–d).

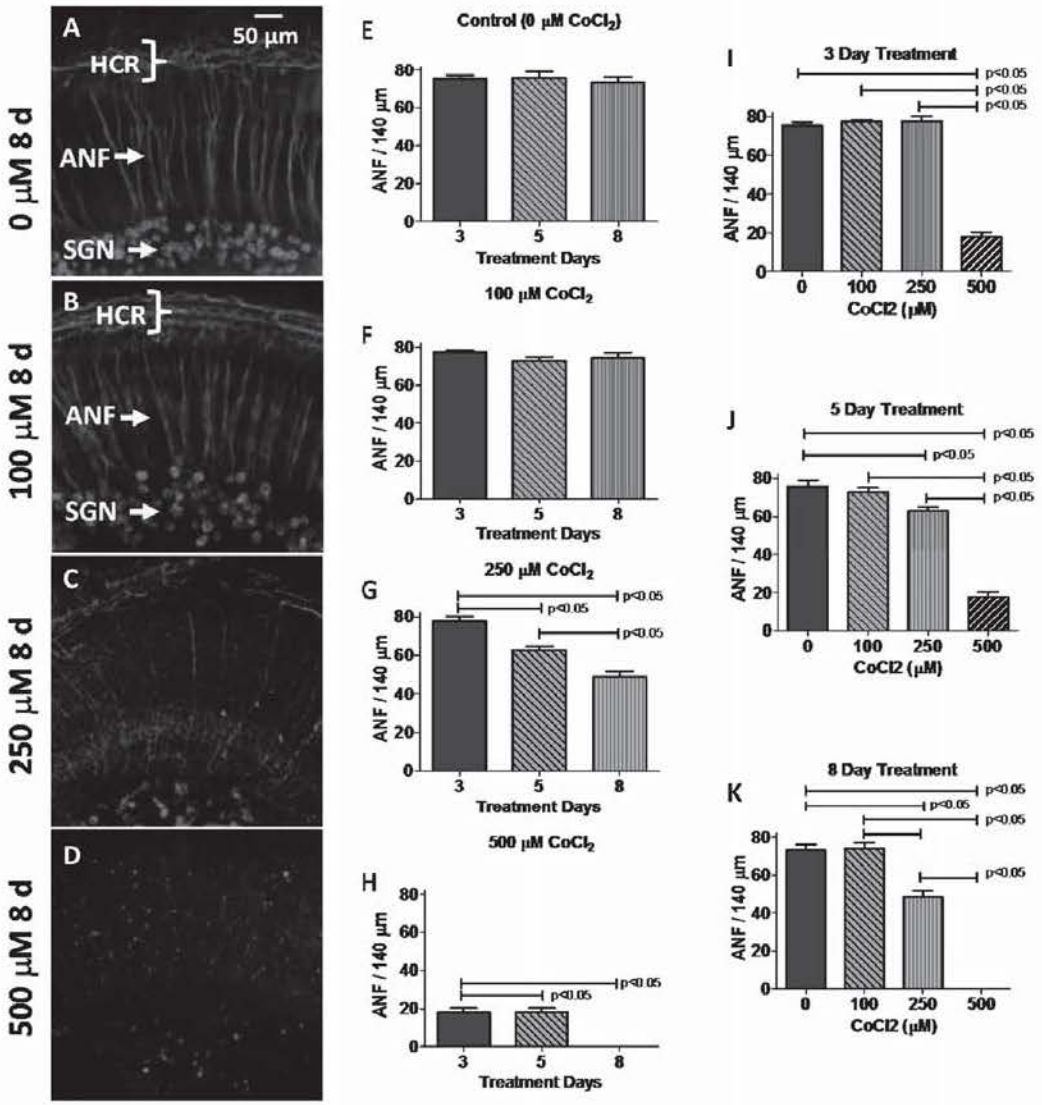

Fig. 3 **a**–**d** Representative photomicrographs of ANF and spiral ganglion neurons (SGN) from the middle of the cochlea after 8 days in culture with 0 (control), 100, 250, or 500 mM $CoCl_2$. Samples immunolabeled with beta tubulin III and TRITC-conjugated secondary antibody. **a** Photomicrograph showing condition of ANF and SGN cultured for 8 days without $CoCl_2$. Note thick fascicles of ANF projecting out from the SGN towards the HCR. Numerous, large round SGN heavily labeled with beta tubulin. **b** ANF and SGN after 8-day treatment with 100 µM $CoCl_2$ were similar to untreated samples. **c** Treatment with 250 µM $CoCl_2$ for 8 days caused a massive reduction in ANF and SGN. **d** Virtually all ANF and SGN were missing after 8-day treatment with 500 µM $CoCl_2$. **e**–**h** Mean (SEM, $n = 4$) numbers of ANF/140 µM after 3-, 5-, or 8-day treatment with 0 (Control), 100, 250, and 500 µM $CoCl_2$. Mean (SEM) ANF/140 µm cultured for 3, 5, or 8 days with 0 (Control), 100, 250, or 500 µM $CoCl_2$; *horizontal lines* in each panel show significant between group difference (Newman–Keuls, $p < 0.05$). **i**–**k** Mean (SEM) ANF/140 µm in cultures treated with 0, 100, 250, or 50 $CoCl_2$ for 3-, 5-, or 8-day treatment durations. *Horizontal lines* identify between group differences that were statistically significant (Newman–Keuls, $p < 0.05$) (Color figure online)

Effect of Treatment Duration on SGN

The numbers of normal SGN and numbers of damage SGN were counted at three locations in the middle of the cochlea and the percentage of normal SGN calculated (see "Materials and Methods" above). Figure 4e shows the mean (SEM) percentages of normal SGN in controls after 3, 5, or 8 days in culture. Approximately 98 % of SGN were normal after 3 and 5 days in culture; however, this declined to roughly 89 % after 8 days in culture. In the

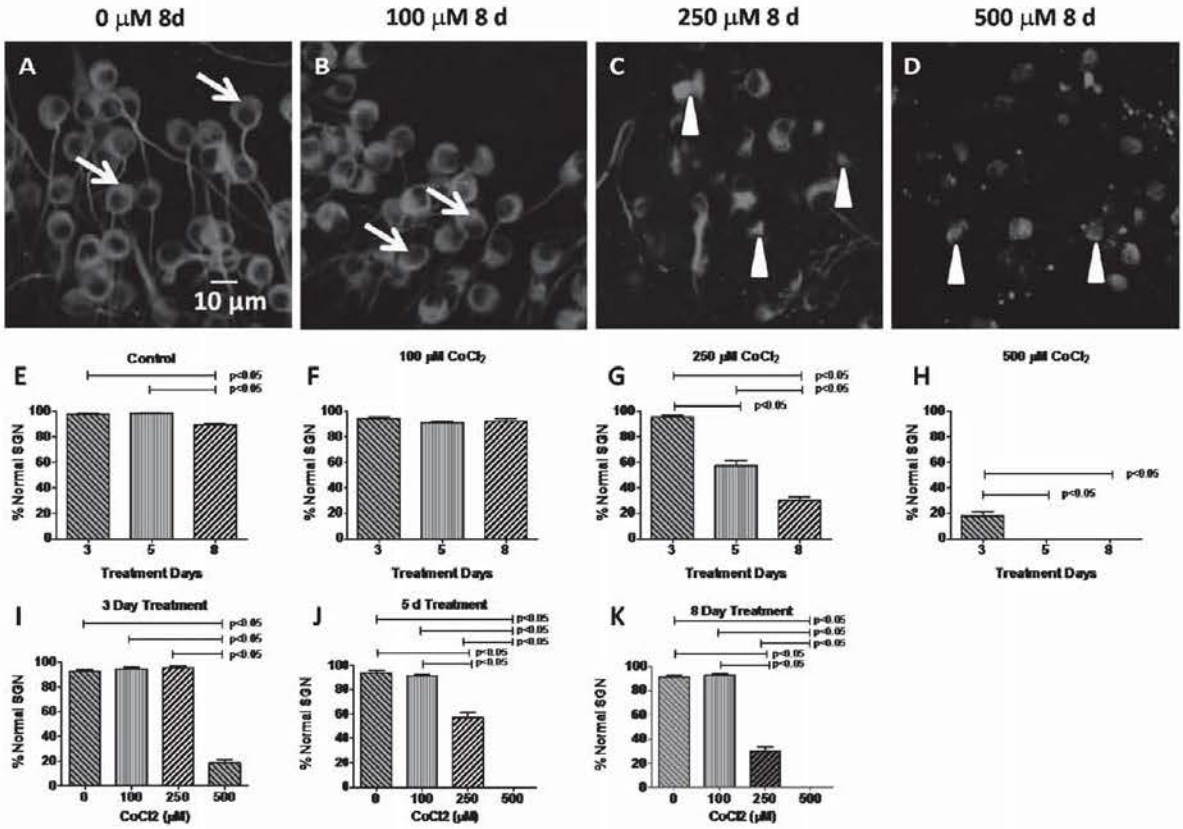

Fig. 4 **a**–**d** Representative photomicrographs of SGN cultured for 8 days with 0, 100, 250, or 500 μM $CoCl_2$. In the Control and 100 μM groups, the large round soma were heavily labeled with an antibody against tubulin except in the nucleus (*yellow arrows*). In the 250 μM and 500 μM groups, fewer SGN were present, and among those still present, the somas were shrunken and the nuclei condensed or fragmented (*white arrowheads*). **e**–**h** Mean (SEM) percentage of normal SGN cultured for 3, 5, or 8 days with 0 (control), 100, 250, or 500 μM $CoCl_2$. **i**–**j** Mean (SEM) percentage of normal SGN treated with 0 (control), 100, 250, or 500 μM $CoCl_2$ for 3, 5, or 8 days. *Horizontal lines* identify between group differences that were statistically significant (Newman–Keuls, $p < 0.05$) (Color figure online)

controls, there was a significant effect of treatment duration on the percentage of normal SGN (one-way ANOVA; $F = 24.72$, 2, 9 df, $p < 0.0002$); a Newman–Keuls post hoc analysis ($p < 0.05$) revealed a significant difference between 5- versus 8-day treatments and 3- versus 8-day treatments. In cultures treated with 100 μM $CoCl_2$, roughly 91–95 % of SGN appeared normal (Fig. 4) and there were no significant differences between the three treatment durations. However, in cultures treated with 250 mM $CoCl_2$, the mean (SEM) percentages of normal SGN declined to roughly 57 and 37 % after 5 and 8 days in culture compared to 95 % after 3 days in culture (Fig. 4f). In the 250 μM $CoCl_2$ group, there was a significant effect of treatment duration (one-way ANOVA, $F = 1.24$, 2, 9 df, $p < 0.001$); a Newman–Keuls post hoc analysis ($p < 0.05$) revealed significant differences between the 8- versus 3-, 8- versus 5-, and 5- versus 3-day treatments. With the 500 μM $CoCl_2$ treatment, the mean (SEM) percentages of normal SGN dropped to roughly 20 % after 3 days of treatment, whereas few if any SGN were normal after 5- or 8-day treatment (Fig. 4h). In the 500 μM $CoCl_2$ group, there was effect of treatment duration (one-way ANOVA, $F = 31.92$, 2, 9 df, $p < 0.0001$); a Newman–Keuls post hoc analysis ($p < 0.05$) showed a significant difference between 3- and 5-day groups and 3- and 8-day groups.

SGN Dose–Response

To assess the effect of $CoCl_2$ dose, the mean (+SEM) percentages of normal SGN were compared for treatment durations of 3, 5, or 8 days. In 3-day treatment group, the mean (SEM) percentage of normal SGN declined to approximately 18 % in the 500 μM $CoCl_2$ group compared to roughly 93 % in the 0, 100, and 250 μM $CoCl_2$ groups (Fig. 4i). There was a statistically significant effect of dose

(one-way ANOVA, $F = 334.2$, 3, 12 df, $p < 0.0001$). The mean (SEM) percentage of normal SGN in the 500 mM group was significantly different from the 0, 100, and 250 mM doses (Newman–Keuls post hoc analysis, $p < 0.05$). In 5-day treatment group, the mean (SEM) percentage of normal SGN was nearly 0 in the 500 μM group and approximately 57 % in the 250 μM group compared to 91–94 % in the 0 and 100 μM groups. In 5-day treatment group, there was a significant effect of dose (one-way ANOVA, $F = 409.7$, 3, 12 df, $p < 0.001$); the 500 μM groups was significantly different from 0, 100, and 250 μM, and the 250 μM group was significantly different from 0 and 100 μM groups (Newman–Keuls post hoc analysis, 3, 12 df, $p < 0.05$). In 8-day treatment group, there were few normal SGN in the 500 μM group and roughly 30 % normal SGN in the 250 μM group compared to approximately 92 % normal SGN in the 0 and 100 μM groups. In 8-day treatment group, there was a significant effect of dose (one-way ANOVA, $F = 504.2$, 3, 12 df, $p < 0.001$); the 500 μM group was significantly different from the 0, 100, and 250 μM groups, and the 250 μM group was significantly different from the 0 and 100 μM groups (Newman–Keuls post hoc analysis, $p < 0.05$).

Co-induced Superoxide

Since Co is known to induce oxidative stress in mitochondria (Battaglia et al. 2009), we used dihydroethidium to determine if 3-day treatment with 0 (control), 250, or 500 μM $CoCl_2$ increased the expression of superoxide in hair cells or SGN (Deng et al. 2013, Nicotera et al. 2004). Our measurements were made at 3 days during the early stage of neurotoxicity prior to significant hair cell or SGN degeneration. Dihydroethidium labeling was largely absent from hair cells (Fig. 5a) and only sporadically seen in SGN (Fig. 5e). Treatment with 250 μM $CoCl_2$ for 3 days resulted in a weak superoxide labeling in hair cells (Fig. 5b) and bright patches of superoxide (red or yellow) in the SGN region (Fig. 5f). Increasing the dose to 500 μM resulted in a substantial increase in superoxide labeling in the HCR (Fig. 5c) and SGN region (Fig. 5g). Little or no superoxide labeling was seen in the support cells surrounding or beneath the hair cells (Fig. 5g), suggesting that the primary targets of cobalt toxicity are the hair cells in the organ of Corti. The gray level measures of dihydroethidium were assessed in the HCR and SGN region of the middle turn of cochlear culture treated for 3 days with 0, 250, or 500 μM $CoCl_2$. The mean ($n = 5$, SEM) superoxide gray level values in the HCR were 14, 22, and 43, respectively for 0, 250, and 500 μM $CoCl_2$ (Fig. 5d). There was a significant effect of dose (one-way ANOVA, $F = 29.4$; 2, 12 df, $p < 0.001$), and a Newman–Keuls post hoc analysis revealed a significant difference ($p < 0.05$) between the 0 and 500 μM treatments. Figure 5h shows the mean ($n = 5$ cultures, +SEM) dihydroethidium gray level values in the SGN region. The mean (SEM) gray scale levels for 0, 250, and 500 μM $CoCl_2$ treated cultures were 13, 28, and 55, respectively. There was a significant effects of dose (one-way ANOVA, $F = 22.8$; 2, 12 df, $p < 0.001$) and a Newman–Keuls post hoc analysis revealed a significant difference ($p < 0.05$) between the 500 μM $CoCl_2$ group versus the 0 and 250 μM groups.

Apoptosis

Since the production of superoxide anion is often associated with caspase-mediated cell death, we used a cell permeable fluorogenic probe to detect activated caspase-3 in the middle turn of cochlear cultures treated for 3 days with 0 (control), 250, or 500 μM $CoCl_2$. Figure 6a–c shows the typical pattern of red caspase-3 labeling in z-axis cross sections through the organ of Corti of samples labeled with To-Pro-3 (blue) which labels the nuclei and Alexa Fluor 488-conjugated phalloidin (green) which labels the cuticular plate and stereocilia of OHC and IHC. Hair cells were largely devoid of caspase-3 labeling in cultures treated with 0 (control) and 250 μM $CoCl_2$; however, robust caspase-3 labeling was present in many OHC and IHC in cultures treated with 500 μM $CoCl_2$. Little or no caspase-3 was seen in the support cells surrounding or beneath the hair cells (Fig. 5g), suggesting that the primary targets of cobalt toxicity are the hair cells in the organ of Corti. Figure 6d–e illustrates the typical pattern of red caspase-3 labeling in SGN stained with To-Pro-3 (blue) and an antibody against β-tubulin (green). A few small patches of caspase-3 were present in cultures treated with 0 (control) or 250 μM $CoCl_2$ (Fig. D, E). However, numerous red or yellow (overlap of red/green) patches of caspase-3 were present in SGN cultured with 500 μM $CoCl_2$. Many of the red- or yellow-labeled SGN in the group treated with the 500 μM $CoCl_2$ had a shrunken soma and a condensed nucleus, morphological features of cells undergoing apoptosis.

Discussion

One of the most import functions of Co is its obligatory role as a component of the vitamin B12 complex discovered almost 70 years ago (Rickes et al. 1948; Becker et al. 1949) with identification of the crystalline structure of the cyano-Co complex. Humans cannot synthesize vitamin B12; therefore, in order to meet their nutritional needs, they are reliant on either direct uptake of cobalamin in foods or via synthesis by microorganisms within the gut. Being a divalent metal, Co can potentially bind to zinc finger proteins and act as an essential cofactor for a number of

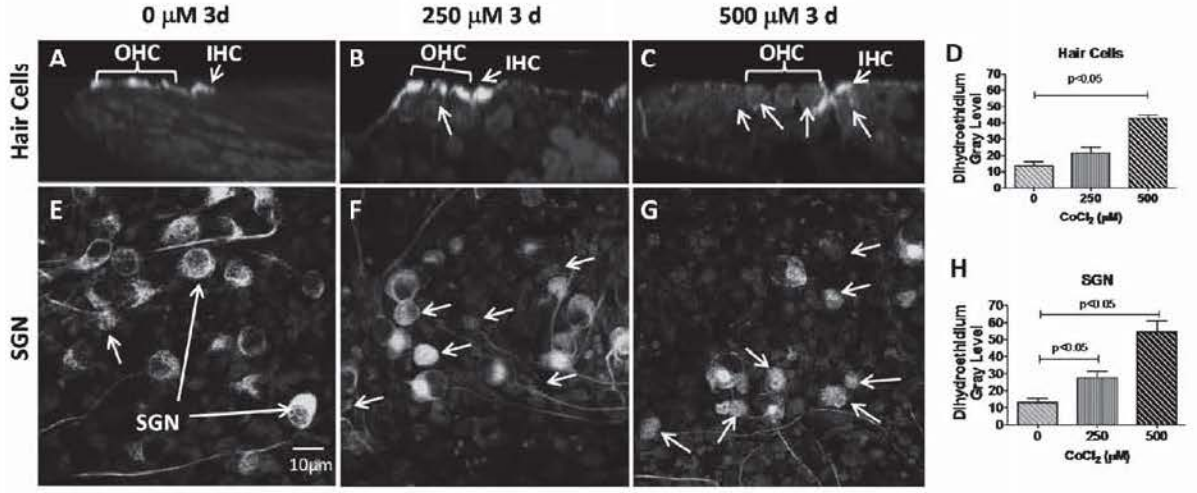

Fig. 5 Representative photomicrographs of 3-day cochlear organotypic cultures labeled with dihydroethidium (*red*) to detect superoxide, To-Pro-3 (*blue*) to label nuclei, Alexa Fluor 488-conjugated phalloidin to label the hair cell stereocilia and cuticular plate and an antibody against β-tubulin with secondary antibody (*green*) to label SGN. Images from cultures treated with 0 (**a**, control), 250 (**b**), or 500 μM (**c**) $CoCl_2$. *Z*-axis radial images through the middle turn of the cochlear cultures showing the cuticular plate of OHC and IHC (*green*), nuclei of hair cells and supporting cells (*blue*) and superoxide labeling (*red*). Little or no superoxide labeling in control hair cells (**a**, 0 μM), a few puncta of superoxide label in the 250 μM $CoCl_2$ group (**b**, *yellow arrow*) and strong superoxide label in the 500 μM group (**c**, *yellow arrows*). **d** Mean (SEM) *gray* level measures of superoxide labeling in hair cell region. Compared to the control group, superoxide label was slightly increased after the 250 μM treatment and significantly increased after the 500 μM treatment. *Horizontal lines* identify between group differences that were statistically significant (Newman–Keuls, $p < 0.05$). Representative photomicrographs showing superoxide labeling in SGNs after 0, 250, or 500 μM $CoCl_2$ treatment. A few puncta of superoxide present in 0 μM control (**f**, *yellow arrow*); many *red puncta* and larger *yellow patches* (overlap of *red/green*) of superoxide in the 250 and 500 μM groups (**f**, **g**, *yellow arrows*). **h** Mean (SEM) *gray* level measures of superoxide in SGN in the 0, 250, and 500 μM groups. *Horizontal lines* identify between group differences that were statistically significant (Newman–Keuls, $p < 0.05$) (Color figure online)

enzymes although by displacing zinc, and it also has the potential to act as an inhibitor of zinc-dependent enzymes and thereby potentiate toxicity (Hartwig 2001). Some if its deleterious effect may also be caused by its actions as a Ca channel antagonist (Barnes and Hille 1989), leading to inhibition of Ca entry and Ca signaling as well as competing with Ca for intracellular Ca-binding proteins (Akbar et al. 2011).

It is estimated that more than a million US workers are exposed to excess Co with the greatest exposure occurring in mining, production of Co powder, tungsten carbide, and other alloys as well as in the manufacturing and processing of hard metals. Excess exposure to Co either caused by failing metal-on-metal implants or occupational exposures can lead to sensory disturbance including hearing loss (Bradberry et al. 2014; Apostoli et al. 2013; Ikeda et al. 2010).

Although hearing loss has been reported in individuals exposed to excess Co, the exact nature of the histopathologies and mechanisms responsible for cell death within the cochlea are poorly understood. To address this issue, we examined the effect of various doses and durations of $CoCl_2$ exposure on the sensory hair cells and SGN in postnatal day 3 rat cochlear cultures. The lowest concentration of $CoCl_2$, 100 μM, failed to cause significant damage to the hair cells or SGN for treatment durations lasting up to 8 days. However, after 5-day treatment with $CoCl_2$ at 250 μM, there was significant and selective loss of OHC in comparison to the IHC in the basal two-third of the cochlea. In addition, there was significant damage to ANF and SGN in the middle of the cochlea. The highest concentration, 500 μM, resulted in total loss of IHC and OHC after 5- and 8-day treatments and significant loss of IHC and OHC in the basal half of the cochlea after 3-day treatment. The highest dose also caused massive loss of ANF and SGN in the middle turn after 3-day treatment and total loss after 8-day treatment. The magnitude of damage to the ANF and SGN in the middle of the cochlea roughly paralleled that seen to the hair cell. As with many other ototoxic drugs, $CoCl_2$ was significantly more toxic to OHC than IHC at intermediate doses and durations (Fig. 2h), consistent with the preferential ototoxic effects of aminoglycosides (Taylor et al. 2008), cisplatin, and other toxic compounds (Tabuchi et al. 2011). We are aware of only one histopathologic study of Co ototoxicity in rabbits which reported on the gross qualitative degenerative changes in the hair cells and SGN (Apostoli et al. 2013) following a single intravenous dose of Co. While these

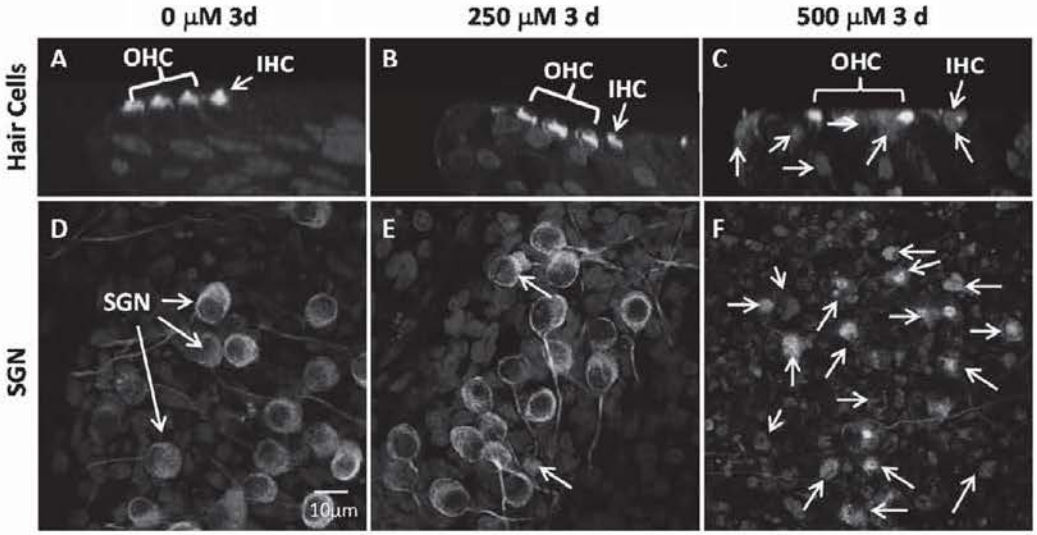

Fig. 6 Representative photomicrographs of the hair cells in the organ of Corti (**a**–**c**) and SGN (**d**–**f**) cultured for 3 days with 0 (control), 250, or 500 μM $CoCl_2$. *Z*-axis images of organ of Corti labeled with Alexa Fluor488-phalloidin (*green*), To-Pro-3 (*blue*) and caspase-3 (*red*). Caspase-3 was largely absent from samples treated with 0 (**a**) or 250 μM $CoCl_2$ (**b**), whereas extensive caspase-3 labeling was evident in IHC and OHC (*yellow arrow*) after treatment with 500 μM with $CoCl_2$ (**c**). SGN samples labeled with caspase-3 (*red*), To-Pro-3 (*blue*), and antibody against β-tubulin (*green*). A few scattered puncta of caspase-3 (*yellow arrows*) present in SGN cultured with 0 (**d**) and 250 μM $CoCl_2$ (**e**); many puncta and large patches of caspase-3 (*yellow arrows*, *red*, or *yellow*) present in SGN cultures treated with 500 μM $CoCl_2$. Caspase-3 was often present in SGN with shrunken soma and condensed nucleus (Color figure online)

results are qualitatively similar to our in vitro observations, no quantitative data were presented regarding the relative amount of IHC vs. OHC loss, the location of hair cell loss along the cochlear tonotopic gradient, or the relationship between $CoCl_2$ dose versus damage to hair cells, ANF, or SGN. Thus, our study provides the first quantitative assessment of Co ototoxicity in vitro. Further work is needed to establish the relationships between Co dose and cochlear damage in vivo.

The dose/duration-response functions established for $CoCl_2$ in vitro can be directly compared to our previous in vitro studies of $MnCl_2$ ototoxicity (Ding et al. 2011b). Mn was slightly more toxic to SGN and ANF than hair cells and induced damage to ANF at concentrations as low as 10 μM, a dose more than ten times lower than that needed for Co to damage ANF. Moreover, significant ANF damage occurred after 48 h treatment with only 50 μM of Mn, much sooner and at lower doses than that seen for Co (Fig. 3). Taken together, these results indicate that Co is substantially less neurotoxic and ototoxic than Mn in postnatal cochlear cultures. Moreover, Co toxicity took longer to develop indicating delayed program of cell death. The pattern of hair cell damage for these two metals was fundamentally different; Mn was more toxic to IHC than OHC, whereas the reverse was true for Co. Mn-induced IHC damage was relatively uniform along the length of the cochlea, whereas IHC loss from Co decreased from the base towards the apex of the cochlea (Fig. 2j). The mechanisms responsible for these differences are unclear but could be related to differences in their cellular uptake, type of oxidative stress, or their effects on cellular metabolism (Hatori et al. 1993).

The mechanisms responsible for Co-induced hair cells or SGN cell death in vitro and in vivo are poorly understood. $CoCl_2$ is a hypoxia memetic which switches cell metabolism from aerobic respiration to anaerobic glycolysis; this leads to the activation and stabilization of hypoxia-inducing factor (HIF) (Regazzetti et al. 2009). Prolonged or high-dose treatment with $CoCl_2$ induces oxidative stress provoking cell death via apoptosis (Jomova and Valko 2011; Lee et al. 2013; Huk et al. 2004). $CoCl_2$ decreases the expression of extracellular superoxide dismutase which scavenges the highly toxic superoxide anion leading to activation of caspase-3 and DNA fragmentation (Adachi et al. 2011). *N*-acetylcysteine, a free radical scavenger and 4-phenyl butyric acid, which enhances extracellular superoxide dismutase, suppressed caspase-mediated cell death. Our results support these prior findings in that cell death induced by $CoCl_2$ promotes the formation of the highly toxic superoxide anion in hair cells and SGN (Fig. 5) as well as activation of caspase-3 (Fig. 6). In this case, production of both superoxide and caspase-3 occurred at concentrations 250 μM Co after 3 days of exposure, suggesting that propagation of these stress signals occur

prior to the observed cell death which is predominantly seen after 5 days in culture at this concentration of Co. The Co-induced switch from aerobic to anaerobic respiration followed by the up regulation of HIF may account for the slow onset of cell death induced by the doses of $CoCl_2$ employed in our study.

It is not known why there are differences in the sensitivity of cells to Co within the cochlea and whether the disparity is caused by differences in Co accumulation in these cells. Absorption of Co is affected by iron and other divalent metals as these metals share common transmembrane transport proteins including divalent metal transporter 1 (DMT1), ZIP8, and ZIP14 (Garrick et al. 2006; Illing et al. 2012; Wang et al. 2012; Pinilla-Tenas et al. 2011). DMT1 comprised four distinct isoforms which differ in their C and N terminals, all of which are transcribed from a common gene (Roth 2006; Garrick et al. 2012). The four isoforms differ in their cellular and subcellular location but essentially have the same affinities for the different deviant metals. ZIP8 and 14 are both members of the SLC39 solute carrier proteins which is capable of transporting a variety of endogenous and exogenous divalent cations. All three transporters have identified to be present in the cochlea. Prior studies have revealed there was almost a total lack of any of the isoforms of DMT1 in hair cells in P3 old rats, although there was a minor presence within hair cells in the adult animal (Ding et al. 2014a). In contrast, both ZIP transporters were detected in both the OHC and IHC, suggesting that these transmembrane proteins may be responsible for uptake of Co in these cells (Ding et al. 2014b). However, since expression of both ZIP transporters was similar in OHC and IHC, it seems unlikely that they are solely responsible for the differences in Co-induced toxicity observed. In this regard, Co has also been reported to be transported into cells via the AMPA glutamate receptor. Since the AMPA receptor is present in rat SGN and ANF terminals beneath IHC and OHC, it is feasible that this receptors may contribute to the overall toxic event provoked by $CoCl_2$ (Kuriyama et al. 1994).

The Co concentrations used to induce toxicity in our cochlear cultures are considerably higher than those seen in plasma of individual with Co toxicity. This is consistent with previous reports showing that the concentrations of other metals needed to induce toxicity in vitro are higher those seen in vivo. For example, concentration of Mn needed to produce toxicity in PC12 cells is in excess of 100 μM, much higher than in vivo (Lin et al. 1993). Similarly, the minimum Cd concentrations required to induce mild toxicity in the rat cochlea was around 100 μM, much higher than that seen in vivo (Liu et al. 2014). Another study reported using concentrations of Co up to 310 μM to examine biomarker gene changes induced by Co in H4-II-E-C3, a rat hepatoma cell line (Permenter et al. 2013). One factor that is likely to account for in vivo versus in vitro differences toxicity is the duration of Co exposure. The half-life of Co in the whole body can be as great as 4 years suggesting toxicity observed in vivo is possibly caused by the prolonged accumulation and exposure of vulnerable cells; such prolonged exposure are nearly impossible to carry out in culture.

In summary, our results show that $CoCl_2$ is toxic to both hair cells and SGN in postnatal day 3 cochlear organotypic cultures. Co-induced hair cell loss progresses from base to apex with increasing dose and duration of treatment with OHC being somewhat more vulnerable than IHC. $CoCl_2$ increased the expression of the highly toxic superoxide anion in hair cells and SGN. This increase was associated with nuclear condensation, soma shrinkage, and the expression of caspase-3 indicative oxidative stress and caspase-mediated cell death. Further studies are need to more fully elucidate the upstream events leading to Co-induced cell death and intervention strategies that can block Co-induced ototoxicity.

Acknowledgments This research was supported in part by a grant from the National Institute for Occupational Safety Health, R01 OH010235.

References

Adachi T, Aida K, Nishihara H, Kamiya T, Hara H (2011) Effect of hypoxia mimetic cobalt chloride on the expression of extracellular-superoxide dismutase in retinal pericytes. Biol Pharm Bull 34:1297–1300

Akbar M, Brewer JM, Grant MH (2011) Effect of chromium and cobalt ions on primary human lymphocytes in vitro. J Immunotoxicol 8:140–149

Apostoli P, Catalani S, Zaghini A et al (2013) High doses of cobalt induce optic and auditory neuropathy. Exp Toxicol Pathol 65:719–727

Barnes S, Hille B (1989) Ionic channels of the inner segment of tiger salamander cone photoreceptors. J Gen Physiol 94:719–743

Battaglia V, Compagnone A, Bandino A, Bragadin M, Rossi CA, Zanetti F, Colombatto S, Grillo MA, Toninello A (2009) Cobalt induces oxidative stress in isolated liver mitochondria responsible for permeability transition and intrinsic apoptosis in hepatocyte primary cultures. Int J Biochem Cell Biol 41:586–594

Becker DE, Smith SE, Loosli JK (1949) Vitamin B12 and cobalt deficiency in sheep. Science 110:71–72

Bradberry SM, Wilkinson JM, Ferner RE (2014) Systemic toxicity related to metal hip prostheses. Clin Toxicol 52:837–847

Deng L, Ding D, Su J, Manohar S, Salvi R (2013) Salicylate selectively kills cochlear spiral ganglion neurons by paradoxically up-regulating superoxide. Neurotox Res 24:307–319

Ding D, Jiang H, Wang P, Salvi R (2007) Cell death after co-administration of cisplatin and ethacrynic acid. Hear Res 226:129–139

Ding D, Jiang H, Salvi RJ (2010) Mechanisms of rapid sensory hair-cell death following co-administration of gentamicin and ethacrynic acid. Hear Res 259:16–23

Ding D, He J, Allman BL, Yu D, Jiang H, Seigel GM, Salvi RJ (2011a) Cisplatin ototoxicity in rat cochlear organotypic cultures. Hear Res 282:196–203

Ding D, Roth J, Salvi R (2011b) Manganese is toxic to spiral ganglion neurons and hair cells in vitro. Neurotoxicology 32:233–241

Ding D, Jiang H, Fu Y, Li Y, Salvi R, Someya S, Tanokura M (2013a) Ototoxic model of oxaliplatin and protection form nicotinamide adenine dinucleotide. J Otol 8:22–30

Ding D, Qi W, Yu D et al (2013b) Addition of exogenous NAD+ prevents mefloquine-induced neuroaxonal and hair cell degeneration through reduction of caspase-3-mediated apoptosis in cochlear organotypic cultures. PLoS One 8:e79817

Ding D, Salvi R, Roth JA (2014a) Cellular localization and developmental changes of the different isoforms of divalent metal transporter 1 (DMT1) in the inner ear of rats. Biometals 27:125–134

Ding D, Salvi R, Roth JA (2014b) Cellular localization and developmental changes of Zip8, Zip14 and transferrin receptor 1 in the inner ear of rats. Biometals 27:731–744

Fu Y, Ding D, Wei L, Jiang H, Salvi R (2013) Ouabain-induced apoptosis in cochlear hair cells and spiral ganglion neurons in vitro. Biomed Res Int 2013:628064

Garrick MD, Singleton ST, Vargas F et al (2006) DMT1: which metals does it transport? Biol Res 39:79–85

Garrick MD, Zhao L, Roth JA, Jiang H, Feng J, Foot NJ, Dalton H, Kumar S, Garrick LM (2012) Isoform specific regulation of divalent metal (ion) transporter (DMT1) by proteasomal degradation. Biometals 25:787–793

Hartwig A (2001) Zinc finger proteins as potential targets for toxic metal ions: differential effects on structure and function. Antioxid Redox Signal 3:625–634

Hatori N, Pehrsson SK, Clyne N, Hansson G, Hofman-Bang C, Marklund SL, Ryden L, Sjoqvist PO, Svensson L (1993) Acute cobalt exposure and oxygen radical scavengers in the rat myocardium. Biochim Biophys Acta 1181:257–260

Huk OL, Catelas I, Mwale F, Antoniou J, Zukor DJ, Petit A (2004) Induction of apoptosis and necrosis by metal ions in vitro. J Arthroplasty 19:84–87

Ikeda T, Takahashi K, Kabata T, Sakagoshi D, Tomita K, Yamada M (2010) Polyneuropathy caused by cobalt-chromium metallosis after total hip replacement. Muscle Nerve 42:140–143

Illing AC, Shawki A, Cunningham CL, Mackenzie B (2012) Substrate profile and metal-ion selectivity of human divalent metal-ion transporter-1. J Biol Chem 287:30485–30496

Jomova K, Valko M (2011) Advances in metal-induced oxidative stress and human disease. Toxicology 283:65–87

Kuriyama H, Jenkins O, Altschuler RA (1994) Immunocytochemical localization of AMPA selective glutamate receptor subunits in the rat cochlea. Hear Res 80:233–240

Lee JH, Choi SH, Baek MW et al (2013) $CoCl_2$ induces apoptosis through the mitochondria- and death receptor-mediated pathway in the mouse embryonic stem cells. Mol Cell Biochem 379:133–140

Lin W, Higgins D, Pacheco M, Aletta J, Perrini S, Marcucci KA, Roth JA (1993) Manganese induces spreading and process outgrowth in rat pheocromocytoma (PC12) cells. J Neurosci Res 34: 546–561

Liu H, Ding D, Sun H, Jiang H, Wu X, Roth JA, Salvi R (2014) Cadmium-induced ototoxicity in rat cochlear organotypic cultures. Neurotox Res 26:179–189

Mates JM, Segura JA, Alonso FJ, Marquez J (2010) Roles of dioxins and heavy metals in cancer and neurological diseases using ROS-mediated mechanisms. Free Radic Biol Med 49:1328–1341

Meecham HM, Humphrey P (1991) Industrial exposure to cobalt causing optic atrophy and nerve deafness: a case report. J Neurol Neurosurg Psychiatry 54:374–375

Nicotera TM, Ding D, McFadden SL, Salvemini D, Salvi R (2004) Paraquat-induced hair cell damage and protection with the superoxide dismutase mimetic m40403. Audiol Neurootol 9:353–362

Pelclova D, Sklensky M, Janicek P, Lach K (2012) Severe cobalt intoxication following hip replacement revision: clinical features and outcome. Clin Toxicol (Phila) 50:262–265

Permenter MG, Dennis WE, Sutto TE, Jackson DA, Lewis JA, Stallings JD (2013) Exposure to cobalt causes transcriptomic and proteomic changes in two rat liver derived cell lines. PLoS One 8:e83751

Pinilla-Tenas JJ, Sparkman BK, Shawki A et al (2011) Zip14 is a complex broad-scope metal-ion transporter whose functional properties support roles in the cellular uptake of zinc and nontransferrin-bound iron. Am J Physiol Cell Physiol 301:C862–C871

Qi W, Ding D, Salvi RJ (2008) Cytotoxic effects of dimethyl sulphoxide (DMSO) on cochlear organotypic cultures. Hear Res 236:52–60

Regazzetti C, Peraldi P, Gremeaux T et al (2009) Hypoxia decreases insulin signaling pathways in adipocytes. Diabetes 58:95–103

Rehfisch P, Anderson M, Berg P, Lampa E, Nordling Y, Svartengren M, Westberg H, Gunnarsson LG (2012) Lung function and respiratory symptoms in hard metal workers exposed to cobalt. J Occup Environ Med 54:409–413

Rickes EL, Brink NG, Koniuszy FR, Wood TR, Folkers K (1948) Vitamin B12, a cobalt complex. Science 108:134

Roth JA (2006) Homeostatic and toxic mechanisms regulating manganese uptake, retention, and elimination. Biol Res 39:45–57

Sha SH, Taylor R, Forge A, Schacht J (2001) Differential vulnerability of basal and apical hair cells is based on intrinsic susceptibility to free radicals. Hear Res 155:1–8

Simonsen LO, Harbak H, Bennekou P (2012) Cobalt metabolism and toxicology—a brief update. Sci Total Environ 432:210–215

Sutto TE (2011) Prioritization of the Oral (Ingestive) hazard of industrial chemicals. Naval Research Laboratory, Washington, DC

Swennen B, Buchet JP, Stanescu D, Lison D, Lauwerys R (1993) Epidemiological survey of workers exposed to cobalt oxides, cobalt salts, and cobalt metal. Br J Ind Med 50:835–842

Tabuchi K, Nishimura B, Nakamagoe M, Hayashi K, Nakayama M, Hara A (2011) Ototoxicity: mechanisms of cochlear impairment and its prevention. Curr Med Chem 18:4866–4871

Taylor RR, Nevill G, Forge A (2008) Rapid hair cell loss: a mouse model for cochlear lesions. J Assoc Res Otolaryngol 9:44–64

Wang CY, Jenkitkasemwong S, Duarte S, Sparkman BK, Shawki A, Mackenzie B, Knutson MD (2012) ZIP8 is an iron and zinc transporter whose cell-surface expression is up-regulated by cellular iron loading. J Biol Chem 287:34032–34043

Wang L, Ding D, Salvi RJ, Roth J (2014) Nicotinamide adenine dinucleotide prevents neuroaxonal degeneration induced by manganese in cochlear organotypic cultures. Neurotoxicology 40:65–74

Yamada K (2013) Cobalt: its role in health and disease. Met Ions Life Sci 13:295–320